GIG Research Institute

JOURNAL OF SUSTAINABLE MINING

Volume 19 | Issue 1 Article 4

2020

Optimising the management of mining waste by means Sentinel-2 imagery: a case study in Joda West Iron and Manganese Mine (India)

RESEARCH PAPER

Optimising the management of mining waste by means of Sentinel-2 imagery: A case study in the Joda West Iron and Manganese Mine (India)

Daniela Guglietta [a,*], Girolamo Belardi [a], Daniele Passeri [a], Rosamaria Salvatori [b], Stefano Ubaldini [a], Barbara Casentini [c], Francesca Trapasso [a]

[a] Institute of Environmental Geology and Geoengineering, Italian National Research Council, Monterotondo, Rome, Italy
[b] Institute of Atmospheric Pollution Research, Italian National Research Council, Monterotondo, Rome, Italy
[c] Water Research Institute, Italian National Research Council, Monterotondo, Rome, Italy

Abstract

A smart economy minimizes the production of waste from mining activities and reuses waste as a potential resource, with the goal of moving towards a near-zero waste society. This paper presents integrated multidisciplinary methodology in order to optimise the management of mining waste. The test site is the Fe–Mn mine in Odisha (India). The mining waste present in the mine has been collected and afterwards X-Ray Powder Diffraction, X-Ray Fluorescence and spectral signatures analysis have been performed for mineralogical, chemical and spectral characterization of the materials. Finally, the classification and mapping of the characterized mining waste was carried out by Sentinel-2A image.

Keywords: mining waste, critical raw materials, remote sensing, iron, manganese, mine management

1. Introduction

Mining and mineral processing wastes are one of the largest chronic waste concerns in the world. Mine wastes are defined as "those waste products originating, accumulating and present at mine sites, which are unwanted and have no current economic value" [1]. The amount of waste produced in mountain top mining environments is staggering. Jamieson [2] reported that North America produces more than 10 times as much solid mine waste as municipal solid waste per capita. According to Eurostat estimations [3], mining and quarrying wastes accounted for more than 720 million tons in 2010, corresponding to 28% of the total waste production in Europe (27 countries).

A number of environmental problems are associated with the disposal of this waste, including ecological losses, downstream contamination and pronounced landscape transformation (e.g., stockpiled waste rock and tailings, subsidence basins, open pits, and removal of overburden rock and topsoil) [4,5]. Due to the continuous need of mining activities to collect raw materials (RMs) to sustain our economy, the deposits of wastes may become orebodies through appropriate innovative management strategies with the aim of minimizing environmental impact and protecting human health.

In this context, mining waste from Fe and Mn ore deposits, which are considered worthless, placed into overburden dumps and are not of interest for the steel industry, due to their low iron content and the need of prior ore dressing, can find a valuable use in many applications other than the mining industry [6]. In 2016–2017, Indian production of iron ore (4th in the world rankings) consisting of lumps, fines and concentrates was 192 million tons, an increase of 22% compared to the previous year, with 52% of the production in the state of Odisha [7]. The amount of waste produced from this kind of mining activity is equal to millions of tons per year.

Received 5 September 2019; revised 10 December 2019; accepted 8 January 2020.
Available online 5 October 2020

* Corresponding author.
E-mail address: daniela.guglietta@igag.cnr.it (D. Guglietta).

https://doi.org/10.46873/2300-3960.1003

In recent years due to difficulties related to accessing RMs, resource depletion, increases in metal prices and environmental pressures, the recovery of critical raw materials (CRMs) from low-grade ore, steel works by-products and industrial waste have become an important issue and a global challenge for present and future generations [8,9]. Although all RMs are important, some of them are of more concern than others in terms of secure and sustainable supply. In 2018 the European Union published an updated list of CRMs for the European Economy [10].

Considering the large amount of mining waste produced worldwide over the years, it is necessary to have accurate information about waste, i.e. exact positioning in the mining area as well as minerals to still be exploited. Additionally, at the time of opening mining activity, the waste chemical and mineralogical composition was ignored or this material was considered below the cut-off grade. Nowadays, advances in innovative technologies and markets mean that deposits of past wastes can be used as sources of RMs [11].

To this end, mining waste mapping is a very useful tool for the management of the mine and remote sensing is a valuable, fast, low cost, simple and non-environmentally invasive technique for optimising in situ sampling strategies, for characterizing exploitable resources, for managing and planning wastes (rich in Fe and Mn) as mineral resources for future use.

In the last decade, the remote sensing technique, applied to multi- and hyper-spectral images, has been used as an effective tool for the mapping of different lithology, ore deposits and mineral resources in several papers [12,13]. Recently, the possibility of open accessing Sentinel images [14] makes the use of remote sensing even more interesting for geological applications [15].

This technique is based on the ability of remote sensors to collect the sun's electromagnetic radiation which is reflected by earth surfaces. The electromagnetic radiation interacts with materials and acquires a characteristic spectral behaviour that can be used to distinguish different materials and to determine their composition.

Geologic remote sensing is based exactly on the possibility to extract quantitative and/or qualitative information on mineral associations from remotely sensed reflectance (or emittance) spectra derived by multispectral images [16].

Many studies have investigated mining waste from airborne, satellite and field spectral data in order to map the spatial distribution of minerals in tailings [17,18].

Generally, a major obstacle is represented by the difficulty of having available, at the same time, satellite images, mineralogical data and geochemical data concerning surface outcropping materials. In situ sampling provides, in fact, an important means to support the validation of remote observations and allows the widening of the information based on a single field measurement to a larger area (i.e. remotely imagery), as well as to build the spectral signature database of the mining waste for multi-temporal monitoring of areas containing mining waste.

In this paper, we propose integrated multidisciplinary methodology to map mine wastes in order to manage and convert them in new valuable and exploitable products. In order to improve current mining waste disposal, we have developed an approach that enables the collection of useful data (chemical, physical and spectral characteristics, location of waste in the mining area), making them into smart data (mapping, minerals to be exploited still, planning of fresh wastes) by means of detailed analyses. As a result, this optimized management valorises mining waste as they are considered as a source of raw materials that new technologies and markets can exploit.

The methodology, tested on wastes produced in the Joda West Iron and Manganese Mine (India), can be summarized by the following steps:

- in situ waste sampling;
- mineralogical and chemical characterization of mining waste by using X-Ray Powder Diffraction (XRPD) and X-Ray Fluorescence (XRF);
- spectral signatures measurements and analysis of mining waste;
- multispectral satellite Sentinel-2A image classification.

This approach can be considered as the first step to promoting the application of economically feasible, socially acceptable, eco-friendly and innovative integrated technologies for the efficient management and sustainable exploitation of mining waste towards a near-zero waste model.

2. Materials and methods

2.1. Study area

Joda West Iron and Manganese Mine (JWIMM) is an opencast mine situated in the North East part of

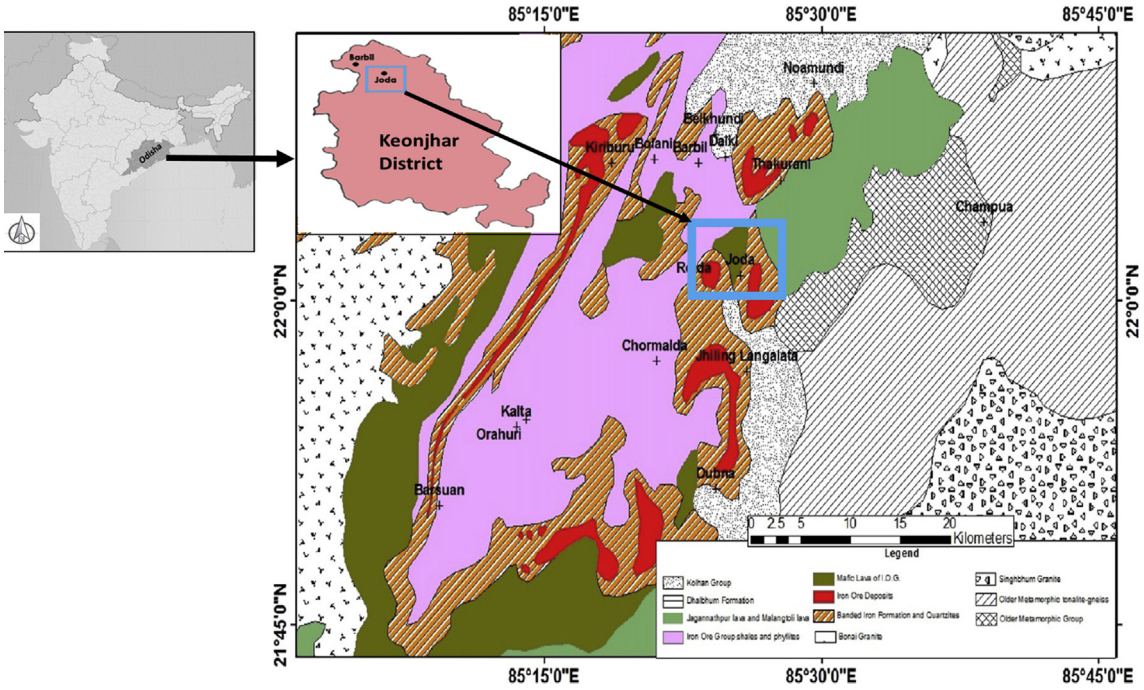

Fig. 1. Study area and geological map of ore bodies in Bonai-Keonjhar belt, Singhbhum Craton, India. Reprinted from 'Reworked manganese ore bodies in Bonai-Keonjhar belt', by [19].

Keonjhar district of Odisha state (India) (Fig. 1) and it has been run by TATA Steel since 1933. The climate is tropical: summer (from April to June) is hot and humid with temperatures hovering around 45 °C and winter is severe (temperature drops below 5 °C). August and September are the wettest months and the annual rainfall varies between 1170 mm and 1500 mm. The study area is characterized by the presence of small hills covered by tropical dry deciduous forests on the higher slopes and shrubs and bushes on the lower level. In geological terms, JWIMM lies in the western portion of the Singhbhum-Odisha craton [19]. The iron ores belong to the Iron Ore Group (IOG) and manganese ore deposits are confined to Shale Formation of the Precambrian IOG. In particular, manganese ore bodies are associated with shales, laterite, chert and, quartzite of the IOG and are distributed within the horseshoe shaped synclinorium, plunging towards NNE over folded towards SW. The shale formation occurs as a core of the synclinorium along Jamda-Koira valley overlying the Banded Iron Formation (BIF – an important volcano sedimentary rock formation of the IOG).

2.2. Sample collection

During the in situ sampling campaign carried out in the second half of November 2017, in different areas of the JWIMM, 37 different mining waste samples (rock as well as debris) were collected (Fig. 2). For each site GPS coordinates, pictures and a brief description of the sampling site were stored and summarized in datasheets.

Whereas, the sub-sampling method (as coning and quartering) was applied to the mining waste samples with the purpose of obtaining a representative sample from a larger one (sampling area). Part of this material was used for spectral measurement and part was grounded for mineralogical analyses. In particular, the subsampled wastes were passed through a 2-mm sieve and grounded in a vibratory grinder (Willy Bleuler Apparatebau Zollikon-Schweiz) for sample characterization in a laboratory.

2.3. Sample characterization

2.3.1. X-Ray Powder Diffraction analysis

XRPD analysis was carried out with a fully automated Bruker AXS D8 Advance diffractometer operating in reflection mode with θ-θ geometry and equipped with high-resolution energy dispersive 1-D Lynxeye XE detector, with an opening of 3° in 2θ. The measurement parameters used were: CuKα, 40 kV, 30 mA, 2.5° soller collimators, 0.6 mm divergence slit, anti-scatter screen, scan angle (2θ) = 0–70°; step width (2θ) = 0.02°; counting time 0.3 s per step. The samples were micronized to under 70 μm in size by a vibrating rotary cup mill at 900 rpm motor speed and a standard 100 ml steel

Fig. 2. In situ sampling campaign. From Google Earth.

crews. The grinding containers incorporate an anvil ring and puck to pulverize the sample by eccentric vibratory action.

Diffraction data was elaborated with DIFFRAC.EVA software and the Crystallography Open Database (COD). The identifiers of the COD can be freely obtained (http://www.crystallography.net/cod/) since COD is an open-access database.

2.3.2. X-Ray Fluorescence analysis

The chemical analyses were carried out by SPECTRO XEPOS ED-XRF elemental analyser optimized for heavy elements with Max power of 50 W and Max voltage of 50 kV. The X-Ray EDS fluorescence spectrometer is equipped with an X-Ray tube with thick binary Pd/Co alloy anode with air-cooling, an adaptive excitation system with optimized filters HAPG (Highly Annealed Pyrolytic Graphite) polarizer for improved sensitivity of elements in the range Na–Cl and a bandpass filter for improved performance for elements in the range K–Mn. The signal detection was carried by an SDD with Peltier cooling with a large detector area (30 mm^2) and active area of 20 mm^2. Spectral resolution (FWHM) $\leq$ 130 eV for Mn Kα and input count rate up to 1,000,000 counts per second. In the instrument, there is a detector filter changer for active pile-up reduction.

Table 1. Wavelengths and bandwidths of Sentinel-2A.

Spatial Resolution(m)	Band Number	Central Wavelength (nm)	Bandwidth (nm)
10	2	496.6	98
	3	560.0	45
	4	664.5	38
	8	835.1	145
20	5	703.9	19
	6	740.2	18
	7	782.5	28
	8a	864.8	33
	11	1613.7	143
	12	2202.4	242

The calibration curves were constructed using international standards and the common linear model developed by Lukas-Tooth and Price [20]. The results were compared with those obtained with the TurboQuant method (XRF Analyzer Pro software) and the SPECTRO procedure calibration model, a combination of the Fundamental Parameter and Extended Compton scattering model with a calibration of the mass attenuation coefficient.

The choice of the best calibration curve for each element was based on the best correspondences of the analytical results with the Given Concentrations of the international standards.

2.3.3. Spectral characterization

In the laboratory, for each waste sample collected in the mine, the spectral signature was recorded using a field hyperspectral spectrometer (FieldSpec FR3 PRO, Analytical Spectral Devices- ASD, Boulder, CO, USA) operating in the visible (VIS), near infrared (NIR) and short wave infrared (SWIR) spectral domains (350 and 2500 nm).

The laboratory spectral measurements were collected using a sensor with field of view of 25° (bare optic fiber probe). The probe was placed approximately 10 cm above the target, nadir viewing

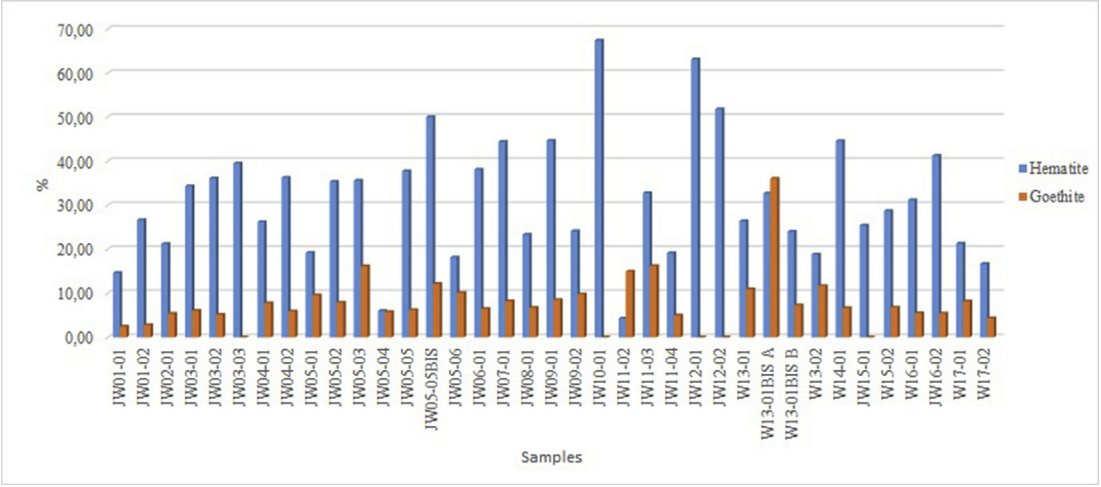

Fig. 3. Hematite and Goethite in Joda West Mine samples.

over the sample, thus analysing (recovering) a surface area of about 15 cm^2; halogen light source (ADS-Lowel Pro-Lamp) was placed approximately 35 cm from the sample (45°viewing). For each measurement, an integration of 50 acquisitions was selected. A white Spectralon® panel (regarded as a Lambertian reflector) was used as a reference to calculate the reflectance of the sample. For each sample, more than four measurements were carried out, rotating the sample by approximately 90° each time to minimize the shadow effects; the reflectance spectra were averaged in order to obtain a single spectrum for each sample. With the aim of guaranteeing good quality analytical data and eliminating problems of the drift of the sensitivity of the instrument, for each sample the reference panel was measured at the beginning and at the end of the measurement session and the estimated error of absolute reflectance was approximately 2%. Furthermore, to use spectral measurement for remote image interpretation, each spectrum was resampled according to the Sentinel-2A spectral band ranges (Table 1).

2.4. Processing of Sentinel-2 satellite image

The Sentinel missions are designed to provide routine observations for operational Copernicus

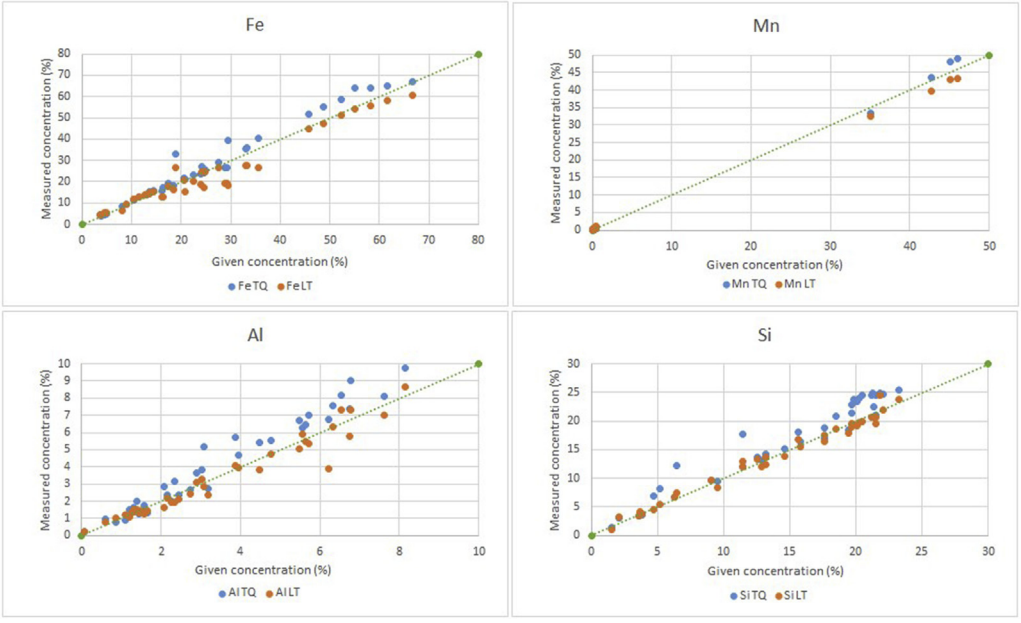

Fig. 4. Lukas-Tooth and Price (LT) vs. SPECTRO procedure (TQ – TurboQuant method) calibration curves.

Table 2. X-Ray Fluorescence analysis partial results.

	Min	Max
Major elements in the samples		
Fe (%)	4.94	49.53
Mn (%)	0.12	46.90
Al (%)	1.29	13.82
Si (%)	1.33	31.85

services and to provide data continuity of ERS, ENVISAT and multispectral missions such as SPOT, Landsat, Aster, etc.

The Sentinel-2A satellite carries a multispectral instrument and has a sun-synchronous 786 km orbit that allows the covering of all the land surfaces and coastal waters between −56 and +84° latitude with a 290 km swath width at a 10 day revisit time at the equator. The mission is primarily designed for global land coverage and associated applications in change detection mapping. Nevertheless, Sentinel-2 multispectral images were utilized for geological applications [17], in order to map the surface mineralogy associated with hydrothermal alteration systems [15,17] as well as the potential areas of acid mine drainage (AMD) generation [21].

In order to map Fe and Mn mining waste, a Sentinel-2A image was acquired of the mine area on November 29, 2017 (the closest overpass to the field sampling survey).

The sampling sites were recognized on the georeferenced Sentinel-2A image and for each site the corresponding spectral signature was extracted by the image and coupled to the spectrum acquired in the laboratory.

To process a multispectral Sentinel-2A image, a Spectral Angle Mapper (SAM) supervised procedure was applied to this data set.

The chosen classifier assigns pixels to classes based on spectral similarity by calculating the angle between the spectra [22], it requires a very small training set and is used by different authors to map ophiolite lithologies [23], the mineralogy of pyrite mine tailings [18], and metasedimentary rocks [7].

Furthermore, to distinguish vegetation from the mining area the Normalized Difference Vegetation Index (NDVI), which is generally used to monitor the state of vegetation with remote sensors, was applied [24–26]. This index is calculated considering the spectral behaviour of vegetation in the visible and near infrared wavelength ranges as shown in Equation (1).

$$NDVI = (NIR\text{-}RED) / (NIR + RED) \quad (1)$$

NDVI ranges from −1 to +1: negative values represent water; values from 0 to 0.3 correspond to bare soil; low, positive values indicate bare soil with vegetation; values higher than 0.35 correspond to vegetation [27,28].

3. Results and discussion

3.1. Mineralogical and chemical characterization of mining waste

The main mineralogical phases of mining waste samples are: Hematite (α-Fe_2O_3), Goethite (α-FeOOH), Muscovite ($KAl_2(AlSi_3O_{10})$ $(F,OH)_2$),

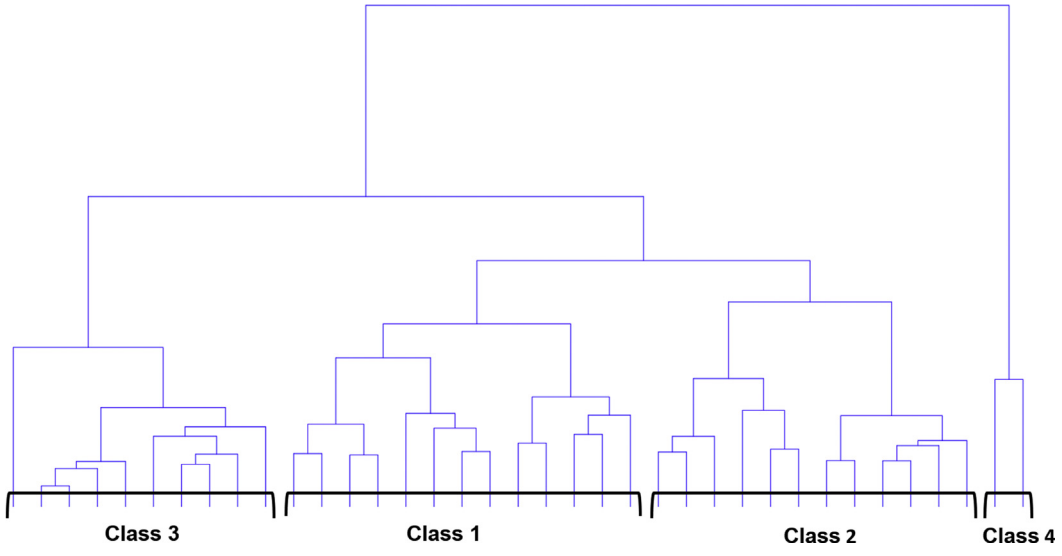

Fig. 5. Cluster analysis results on the percentage values of Fe and Mn and the spectral reflectance values of each sample. The boxes represent four classes used as input to classify Sentinel-2A image.

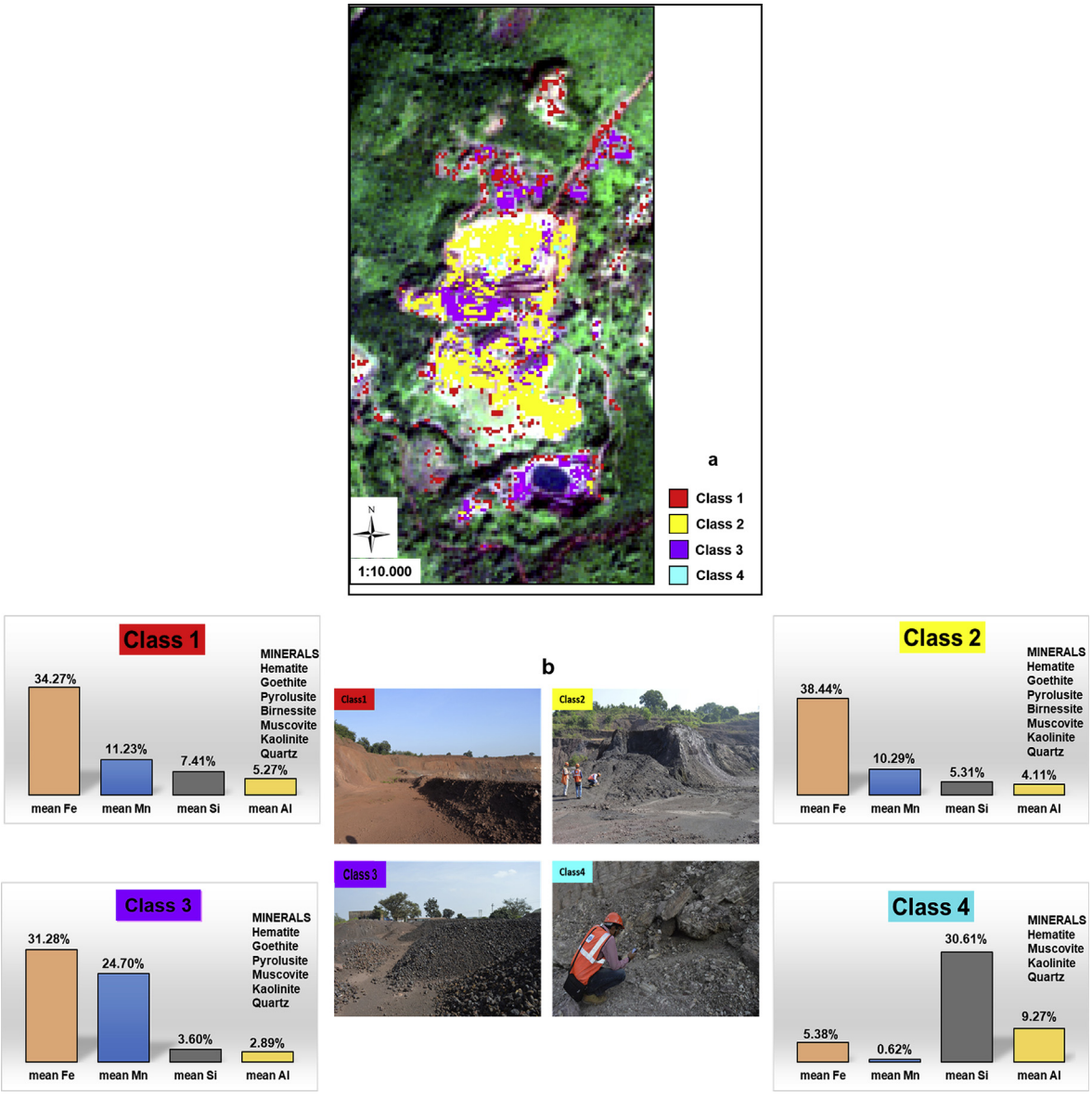

Fig. 6. Mining waste deposit map that shows the spatial distribution of the four mining waste classes (a) and the different percentage of minerals in each class (b). The four classes have been overlaid on Sentinel-2A image in true colour (Red: band 4; Green: band 3; Blue: band 2; spatial resolution: 10 m).

Kaolinite ($Al_2Si_2O_5(OH)$), Quartz (SiO_2) and Pyrolusite (MnO_2). The main iron phases (Hematite and Goethite) are present in variable percentages in the samples with maximum values of 67.41% and 36.04% and minimum values of 4.26% and 2.41%, respectively (Fig. 3). The main manganese phase (Pyrolusite) is present in variable percentages in the samples with a maximum value of 26.00% and minimum value of 2.67%.

For some iron phases (Akaganeite (β-FeOOH), Lepidocrocite (γ-FeOOH), Feroxyhyte (δ′-FeOOH), and Ferrihydrite ($Fe_5HO_8{-}4H_2O$)), it is not possible to establish whether they are actually present in a small percentage (1–2%) due to the noisy background of the diffraction spectra. Maghemite (γ-Fe_2O_3) and Magnetite (Fe_3O_4) have their main peaks hidden by diffraction peaks of other phases, so they have not been included in the semi-quantitative analysis.

Fig. 4 shows a comparison between the calibration curves of some elements of particular interest constructed using the Lukas-Tooth and Price common linear model and those obtained with the SPECTRO procedure. Table 2 shows the minimum and maximum values of the most abundant elements present in the samples.

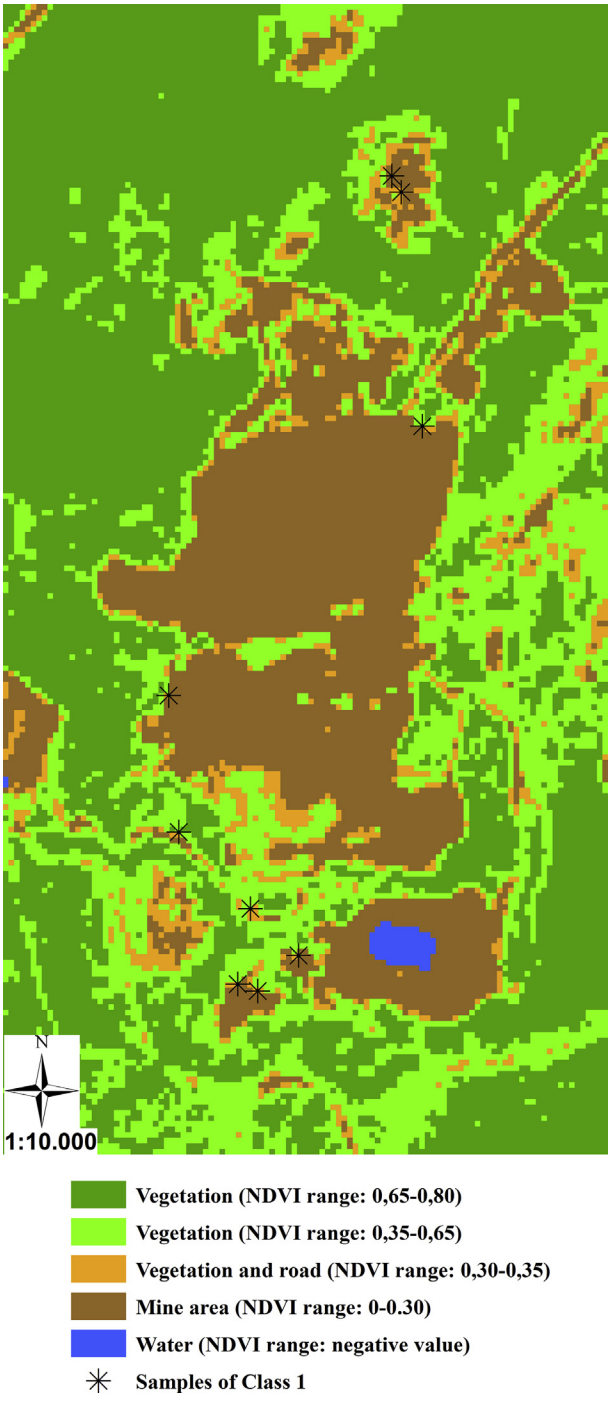

Fig. 7. The NDVI output image: the presence of vegetation and mining wastes dumped by the roadside is highlighted in orange. Asterisks represent samples of Class 1 used as input to classify Sentinel-2.

3.2. Fe and Mn waste map by means of Sentinel-2A

Considering the XRF and XRPD results, in order to characterize mining waste by remotely image this research was focused on elements and minerals with a percentage higher than 5%: firstly, those with a presence of Fe and Mn, and then also Si and Al.

In particular, iron wastes are broadly reused in civil engineering constructions [29–31] and in water treatment for Arsenic removal [32–34]. Additionally, these samples are rich in manganese (20–50%) and Mn recovery is interesting because this element is included in the list of CRMs for the European Economy [10].

Moreover, a number of studies have been conducted on the use of satellite and airborne sensors for Fe and Mn mineral mapping from being 'spectrally active' [17,35–38]. In this paper, to identify samples of mining waste with similar mineralogical, chemical and spectral behaviour, a hierarchical cluster analysis using the Euclidean distance and the average linkage between groups criterion (UPGMA) was performed [39]. The percentage values of Fe and Mn, the reflectance values derived by Sentinel-2A image and reflectance values collected in the laboratory of each sample were used as input data.

The result of the cluster analysis is shown in Fig. 5 by means of a dendrogram that highlighted 4 groups of samples. These groups were analysed by the coupling of in situ data description (i.e. site characteristics, X,Y coordinate by GPS and pictures) and the results of mineralogical, chemical and spectral characterization. Moreover, cluster analysis results highlighted that all class samples were collected in very morphologically and topographically similar mining areas (roadside with sparse vegetation, open space, stocks, no longer exploited mining area).

The Sentinel spectra of each detected group was used as a training set to classify the Sentinel-2A image.

In particular, the four classes identify four distinct typologies of areas containing mining waste: Class 1 – waste dumped by the roadside with the presence of sparse vegetation; Class 2 – waste accumulated in open space; Class 3 – waste deposits of lower-grade ores; Class 4 – waste abandoned in a closed mine.

The results of Spectral Angle Mapper (SAM) classification were represented in a map of mining waste deposits (Fig. 6a) that shows the spatial distribution of the four mining waste classes, thus identifying waste deposit areas with different mean percentages of Fe and Mn, and then also Si and Al (Fig. 6b).

The accuracy of the classification was as follows: user's accuracy = 94.81%; producer's accuracy = 95.23%; overall accuracy = 95.88%; k = 0.806.

Moreover, the result of the NDVI computation were merged with SAM classification results to verify the presence of vegetation. In particular, the NDVI output image (Fig. 7) highlights the presence of vegetation in Class 1, indicating that these wastes are exposed for a longer period of time than compared to Class 2, which is characterized by the steady accumulation of extractive wastes. Finally, Class 3 is very rich in Fe and Mn, but these deposits of wastes are not of interest for the steel industry because they need of mineral preprocessing. Class 4 consists of waste deposits with lower Fe and Mn content.

Given the importance of the possible reuse of mining waste in large areas, the waste deposits map (Fig. 6 a) represents a basic tool to detect waste deposits, which are homogeneous in terms of Fe and Mn, as well as an instrument for optimising the future planning and managing of the mining waste deposit arrangement in Joda West mine areas.

In fact, these mining waste deposits can be valorised and considered as new orebodies by having their exact positioning and the minerals contained to still be exploited. Furthermore, all collected data can be used to unlock the potential raw materials in further reuse and recycle processes and to reduce the environmental impact of waste products accumulated at mine sites.

4. Conclusions

A smart economy minimizes the production of waste and promotes its reuse as a resource for a new industrial process, which enables the movement towards a near-zero waste society with reduced environmental impacts and improved quality of life.

Nowadays, the recycling and reuse of mining waste is very attractive when looking at reducing the environmental impact of mining activities, increasing protection for human health and finding suitable solution with an economic value since cost-benefit analysis is always the ultimate driver in terms of the feasibility of a specific reuse technology.

Multidisciplinary research on mine wastes focuses on understanding their character, stability, impact, remediation, and reuse. The importance of continuing this approach in order to better understand and sustainably manage the huge quantities of historic, contemporary and future mine wastes, is unquestionable, also when considering the trend to exploit larger deposits of lower-grade ores.

The XRPD and XRF analysis highlighted the presence of wastes rich in Fe and Mn that could be reused for extracting exploitable RMs. For example, the recovery of quartz sand for concrete production and kaolin for industrial applications (automotive, ceramic, agriculture); manganese in the amount of 20–50% is often measured in waste samples and this makes these materials interesting for Mn recovery.

Remote sensing techniques that have lower costs than field methods for the characterization of exploitable resources (such as iron and manganese deposits) exposed on the Earth's surface, can be used to rapidly map large areas. The ESA Copernicus Program provides free multispectral images and launched the Sentinel-2A satellite on June 23, 2015, therefore, this paper present one of the first study in which the image is used to characterize and to map the mining waste combining mineralogical and spectral characteristics into an Fe and Mn deposit map.

The map obtained (Fig. 7) enables not only the recognition of the areas with the highest concentration of reusable wastes but also can help to efficiently sort the waste that will be produced, storing it in homogeneous areas.

Moreover, the datasheets of samples containing all the information from in situ sampling and laboratory analysis could be used for developing a preliminary database of mining waste. This database could be an important step to organizing the multidisciplinary information regarding mine wastes and it could be a relevant tool for optimising the waste management as well as for further research in the field of mining waste reusing and recycling. It will also be the key to knowing the chemical, mineralogical and spectral characteristics of the mine wastes and could be updated and implemented with results obtained by further innovative analysis.

Finally, the possibility of providing, at the same time, laboratory spectral signatures associated with mineralogical and geochemical data concerning surface-outcropping materials enabled the creation of a spectral library of mining waste, which could be used in further satellite image classifications.

Conflicts of interest

None declared.

Ethical statement

Authors state that the research was conducted according to ethical standards.

Funding

TECO Project – Technological eco-innovation for the quality control and the decontamination of polluted waters and soils. Reference: EuropeAid/135-474/DD/ACT/IN, "EU-India Research and Innovation Partnership".

Acknowledgments

The authors are grateful to the staff of TATA Steel for providing general support during fieldwork.The authors are grateful to TECO Project ICI+/2014/342–817 – Technological Eco – Innovations for the Quality Control and the Decontamination of Polluted Waters and Soils, for funding this research.

References

[1] Lottermoser BG. In: Mine wastes: Characterization, treatment and environmental impact. 3rd ed. Berlin Heidelberg: Springer-Verlag; 2010.
[2] Jamieson HE. Geochemistry and mineralogy of solid mine waste: Essential knowledge for predicting environmental impact. Elements 2011;7(6):381–6.
[3] Eurostat European Commission. Energy, transport and environment indicators, Eurostat Pocketbooks. Luxembourg: European Union; 2009.
[4] Hudson-Edwards KA, Jamieson HE, Lottermoser BG. Mine wastes: Past, present, future. Elements 2011;7(6):375–80.
[5] Palmer MA, Bernhardt ES, Schlesinger WH, Eshleman KN, Foufoula-Georgiou E, Hendryx MS, et al. Mountain top mining consequences. Science 2010;327(5962):148–9.
[6] Rao SR. Resource recovery and recycling from metallurgical wastes. Amsterdam: Elsevier; 2006.
[7] Ministry of Mines. Annual report 2017-2018, government of India, shastri bhawan, dr. Rajendra prasad road, New Delhi-110001. Available at: https://mines.gov.in/writereaddata/UploadFile/Mines_AR_2017-18_English.pdf; 2017-2018.
[8] Lottermoser BG. Recycling, reuse and rehabilitation of mine wastes. Elements 2011;7(6):405–10.
[9] Yamaguchi T, Nagano H, Murai R, Sugimori H, Sekiguchi C, Sumi I. Development of Mn recovery process from waste dry cell batteries. J Mater Cycles Waste Manag 2018;20(4):1909–17.
[10] European Commission. Report on critical raw materials and the circular economy, Vol. 1. Brussels: European Union; 2018.
[11] Scoble M, Klein B, Scott Dunbar W. Mining waste: Transforming mining systems for waste management. Int J Min Reclamat Environ 2003;17(2):123–35.
[12] Asadzadeh S, de Souza Filho CR. A review on spectral processing methods for geological remote sensing. International J Appl Earth Obs Geoinf 2016;47:69–90.
[13] Van der Meer FD, van der Werff HMA, van Ruitenbeek F-JA, Hecker CA, Bakker WH, Noomen MF, et al. Multi- and hyperspectral geologic remote sensing: A review. International Journal of Applied Earth Observation and Geoinformation 2012;14:112–28.
[14] Berger M, Moreno J, Johannessen JA, Levelt PF, Hanssen RF. ESA's sentinel missions in support of Earth system science. Remote Sen Environ 2012;120:84–90.
[15] Van der Werff HMA, van der Meer FD. Sentinel-2A MSI and Landsat 8 OLI provide data continuity for geological remote sensing. Remote Sens 2016;11:883–99.
[16] Mustard JF, Sunshine JM. Spectral analysis for earth science investigation: Investigations using remote sensing data. Remote Sens Earth Sci: Manual Remote Sens 1999;3:251–307.
[17] Van der Meer FD, van der Werff HMA, van Ruitenbeek F-JA. Potential of ESA's Sentinel-2 for geological applications. Remote Sens Environ 2014;148:124–33.
[18] Zabcic N, Rivard B, Ong C, Mueller A. Using airborne hyperspectral data to characterize the surface pH and mineralogy of pyrite mine tailings. Int J Appl Earth Obs Geoinf 2014;32:152–62.
[19] Mishra P, Mishra SK, Singh PP, Mohapatra BK. Reworked manganese ore bodies in Bonai-Keonjhar belt, Singhbhum Craton, India: Petrology and genetic study. Ore Geol Rev 2016;78:361–70.
[20] Lucas-Tooth HJ, Price BJ. A mathematical method for the investigation of inter-element effects in X-ray fluorescent analyses. Metallurgia 1961;64:149–52.
[21] Mielke C, Boesche N, Rogass C, Kaufmann H, Gauert C, de Wit M. Spaceborne mine waste mineralogy monitoring in South Africa, applications for modern push-broom missions: hyperion/OLI and EnMAP/sentinel-2. Remote Sens 2014;6(8):6790–816.
[22] Kruse FA, Lefkoff AB, Boardman JW, Heidebrecht KB, Shapiro AT, Barloon PJ, et al. The spectral image processing system (SIPS)-interactive visualization and analysis of imaging spectrometer data. Remote Sens Environ 1933;44(2–3):145–63.
[23] Van der Meer FD, Vazquez-Torres M, Van Dijk PM. Spectral characterization of ophiolite lithologies in the Troodos Ophiolite complex of Cyprus and its potential in prospecting for massive sulphide deposits. Int J Remote Sens 1997;18(6):1245–57.
[24] D'Odorico P, Gonsamo A, Damm A, Schaepman ME. Experimental evaluation of Sentinel- 2 spectral response functions for NDVI time-series continuity. IEEE Trans Geosci Rem Sens 2013;51(3):1336–48.
[25] Frampton WJ, Dash J, Watmough G, Milton EJ. Evaluating the capabilities of Sentinel- 2 for quantitative estimation of biophysical variables in vegetation. ISPRS J Photogrammetry Remote Sens 2013;82:83–92.
[26] Jönsson P, Cai Z, Melaas E, Friedl MA, Eklundh L. A method for robust estimation of vegetation seasonality from Landsat and Sentinel- 2 time series data. Remote Sens 2018;10:635–48.
[27] Defries RS, Townshend JRG. NDVI- derived land cover classifications at a global scale. International Journal of Remote Sens 1994;15(17):3567–86.
[28] Mandanici E, Bitelli G. Preliminary comparison of Sentinel- 2 and Landsat 8 imagery for a combine use. Remote Sens 2016;8:1014–24.
[29] Sant'ana Filho JN, Da Silva SN, Cordeiro Silva G, Castro Mendes J, Fiorotti Peixoto RA. Technical and environmental feasibility of interlocking concrete pavers with iron ore tailings from tailings dams. J Mater Civ Eng 2017;29(9):395–412.
[30] Yellishetty M, Karpe V, Reddy EH, Subhash KN, Ranjith PG. Reuse of iron ore mineral wastes in civil engineering constructions: A case study. Resour Conserv Recycl 2008;52:1283–9.
[31] Ismail ZZ, Al-Hashmi EA. Reuse of waste iron as a partial replacement of sand in concrete. Waste Manag 2007;28:2048–53.
[32] Antelo J, Avena M, Fiol S, López R, Arce F. Effects of pH and ionic strength on the adsorption of phosphate and arsenate at the goethite–water interface. J Colloid Interface Sci 2005;285(2):476–86.
[33] Cundy AB, Hopkinson L, Whitby RL. Use of iron-based technologies in contaminated land and groundwater remediation: A review. Sci Tot Environ 2008;400(1–3):42–51.
[34] Zhang M, Dai M, Xia L, Song S. Comparison of arsenic adsorption on goethite and amorphous ferric oxyhydroxide in water. Water Air Soil Pollut 2017;228(11):427.
[35] Clark RN. Spettroscopy of Rocks and Minerals, snd principles of spectroscopy. In: Rencz AN, editor. Remote sensing for the earth sciences: Manual of remote sensing. 3rd ed. John Wiley & Sons; 1999.
[36] Harris JR, McGregor R, Budkewitsch P. Geological analysis of hyperspectral data over southwest baffin island:

Methods for producing spectral maps that relate to variations in surface lithologies. Can J Rem Sens 2010;36(4): 412–35.
[37] Nair AM, Mathew G. Effect of bulk chemistry in the spectral variability of igneous rocks in VIS-NIR region: Implications to remote compositional mapping. Int J Appl Earth Obs Geoinfor 2014;30:227–37.
[38] Suman Babu P, Majumdar TJ, Bhattacharya AK. Study of spectral signatures for exploration of Bauxite ore deposits in Panchpatmali, India. Geocarto Int 2015;30(5):545–59.
[39] Legendre P, Legendre L. In: Numerical ecology. 3rd ed. Amsterdam: Elsevier; 2012.